Advances in Research
3(5): 477-487, 2015, Article no.AIR.2015.043
ISSN: 2348-0394

SCIENCEDOMAIN *international*
www.sciencedomain.org

Comparative Design for Improved LQG Control of Longitudinal Flight Dynamics of a Fixed-Wing UAV

B. K. Aliyu[1*], A. M. Chindo[1], A. O. Opasina[1] and Alih Abdulrahaman[1]

[1]Federal Ministry of Science and Technology (FMST), National Space Research and Development Agency (NASRDA), Centre for Space Transport and Propulsion (CSTP) Epe, Lagos State, Nigeria.

Authors' contributions

This work was carried out in collaboration between all authors. Authors BKA designed the study wrote the first draft of the manuscript. Author AMC verified all DATCOM results and edited the first drafted manuscript. Author AOO evaluated the practical implications for control requirement and verified all MATLAB/Simulink results. Author AA re-checked all MATLAB/Simulink results and managed the literature search. All authors read and approved the final manuscript.

Article Information

DOI: 10.9734/AIR/2015/14174
Editor(s):
(1) Shi-Hai Dong, Department of Physics, School of Physics and Mathematics National Polytechnic Institute, Building 9, Unit Professional Adolfo Lopez Mateos, Mexico.
Reviewers:
(1) Anonymous, Brasilia University, Brazil.
(2) Anonymous, Dalian Maritime University, China.
(3) Anonymous, Nanjing University of Science and Technology, Nanjing, China.
(4) Marcelo Becker, Mechanical Engineering Department / São Carlos School of Engineering / University of São Paulo / Brazil.
Complete Peer review History: http://www.sciencedomain.org/review-history.php?iid=757&id=31&aid=7062

Original Research Article

Received 22nd September 2014
Accepted 5th November 2014
Published 22nd November 2014

ABSTRACT

This paper explores the design, simulation and analysis of three novel Linear Quadratic Gaussian (*LQG*) control system for a Longitudinal dynamic of a fixed wing mini Unmanned Aerial Vehicle (UAV). Modelling results for the small UAV using Aircraft DIGITAL DATCOM® are presented. The novelty of the design is from the stand point of the *Kalman Filter*, with *Kalman gain* obtained from the solution to a *Differential Riccati Equation* (DRE) rather than the popular *Algebraic Riccati Equation* (ARE). The formulated DRE to the Kalman filter design is solved as an Initial Value Problem (IVP) in the MATLAB/Simulink® using explicit algorithm *ode45.* The algorithm converges to a solution of interest with 6671*steps*. Each step has a covariance matrix hence a different *Kalman gain* value as the solution tries to converge, after 10 seconds of simulation. Three of 6671 *step* values are selected based on the observed trajectory of the *Kalman gain* matrix and the time for the set-point tracking control of the pitch angle to reach a *steady-state value*. Three of these Kalman

**Corresponding author: E-mail: aliyu_bhar@yahoo.com, kisabo.aliyu@cstp.nasrda.gov.ng;*

gains obtained were used in the design of the linear Kalman filter, which serves as the observer for the Linear Quadratic Regulator (*LQR*), hence the improved *LQG* controllers. Comparison is made between the three improved *LQG* controllers and the *LQG* controller on the bases of step response characteristics and robustness. Using the robustness properties of the Kalman filter as a benchmark, simulation result shows that all the three improved *LQG* controllers outperform the *LQG*.

Keywords: LQG; improved LQG; MATLAB/Simulink; Differential Riccati Equation.

1. INTRODUCTION

Recently there has been a tremendous growth of research emphasizing control of unmanned aerial vehicles (UAVs) either in isolation or in teams. As a matter of fact, UAVs increasingly find their way into military and law enforcement applications (e.g. Reconnaissance, remote delivery of urgent equipment/material, resource assessment, environmental monitoring, battlefield monitoring, ordinance delivery, etc.). This trend will continue in the future, as UAVs are poised to replace the human-in-the-loop during dangerous missions. Civilian applications of UAVs are also envisioned such ascrop dusting, geological surveying, search and rescue operations, etc. [1]

UAVs have become popular as flight test platforms in the domain of flight control research. The vehicles are attractive due to their compact dimensions, low cost and limited risk of damage or harm in the event of failure. An important task for the development of UAV flight test platforms is modelling and identifying the aircraft dynamics. Accurate models of UAV flight dynamics are generally unavailable due to the custom design of the airframes. However, such models are required to characterize aircraft behaviour and determine stability and performance properties [2] before effective control.

Borkar and Mitter [3] introduced the problem of *LQG* control under communication constraints. Furthermore, Tatikonda, Sahai and Mitter [4] examined the *LQG* performance over both noisy and noiseless channels. The solution of the *LQG* control problem is one of the most celebrated results in the control and systems field. Kalman Filter is an estimator for the Linear Quadratic Problem (*LQR*) - thus the *LQG* controller. Both the *LQR* and Kalman filter have excellent properties of robustness but the combination of both in the *LQG* formulation has no guaranteed robustness.

This paper describes the designs and analysis of the *LQG* problem with three improved versions [5] applied to a UAV. First, a systematic procedure for modelling and analysis used to determine the flight dynamics of the Ultra Stick 25e. This UAV is commercially available and serves as the primary flight test vehicle for the University of Minnesota UAV flight control research group [6]. The Ultra Stick 25e is a small, low-cost, fixed-wing, radio controlled aircraft. It is equipped with standard elevator, aileron and rudder control surfaces as shown in Fig. 1. The aircraft is powered by an electric motor that drives a propeller.

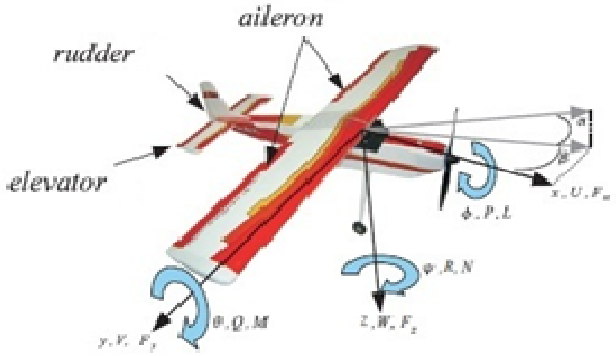

Fig. 1. Ultra stick 25e mini UAV

The movement of an aircraft can be modelled with a linear time invariant dynamic system, which must be controlled by a flight controller. This study contains the synthesis and analysis of the stability and other qualitative control parameters for flight control.

Once key variables of the aircraft's body and lifting surfaces have been defined, as shown in Table 1, Aircraft DIGITAL DATCOM® was used to calculate the aircrafts aerodynamic stability derivatives and control derivatives over a range of flight conditions [7]. These coefficients make up the linear mathematical model, which serves as the bases for the design of the *LQG* controller and the three improved versions.

1.1 Aerodynamic Model of the UAV

Dimensionless aerodynamic coefficients are associated with the stability and control derivatives in terms of independent parameters have been widely used to represent the aerodynamic characteristic of an aircraft for subsonic flight [8]. For pitch plane, these are:

$$C_D = C_{D_0} + k\alpha_e^2\alpha^2,$$
$$C_L = \frac{C_{L_0}}{\sqrt{1-M_\infty^2}}, \quad (1)$$
$$C_m = \frac{C_{m_0}}{1-M_\infty^2},$$

where, α_e is the equilibrium incidence angle of attack, k is a dimensionless constant depending on the body shape and flow regime. C_L and C_m are based on *Prandtl-Glauert* correction (compressibility correction), and the free stream *Mach* number which for this research is $M_\infty = 0.3$. Hence, DATCOM® gave the results in Fig. 2.

It is of great interest to note that from Fig. 2, the stall angle of attack is 12^0 hence a control engineer will ensure that throughout the flight regime such angle-of-attack is not exceeded.

The remaining sections of this paper are organized as follows: A general fixed-wing aircraft flight dynamics model structure is presented in III. Also, properties of the Ultra Stick 25e and the preliminary analysis required to obtain a baseline model of the flight dynamics are described in this section. The *LQG* control design is presented in section IV. Section V details the improved *LQG* control system design with simulation results.

1.2 Fixed-Wing Aircraft Flight Dynamics

The equations of motion for conventional fixed-wing aircraft can be derived analytically from the Newton-Euler equations, where the main task is to determine expressions for the external forces. These forces include gravitational forces, propulsion forces, and aerodynamic forces. The resulting equations of motion are nonlinear and coupled. A linear model is derived by assuming small perturbations from equilibrium. The nonlinear equations of motion are linearized about a particular equilibrium flight condition, or operating point. An operating point is defined by airspeed, altitude, climb rate and turn rate.

Table 1. Physical properties of the mini-UAV

	Description	Value
A	Wing reference area	$0.31m^2$
b	Wing span	$1.27m$
$\overline{c}$	Wing chord	$0.25m$
m	Gross weight	1.9kg
m_c	Mass of camera	$0.25kg$

The simplest form of the equations of motion is taken in the body axis reference frame of the aircraft and assumes a flat Earth coordinate system. Twelve states are required to describe the aircraft rigid-body dynamics: Three inertial positions (X,Y,Z), three body-axis velocities (u,v,w), three attitude angles (ϕ, θ, φ),and three body-axis angular rates (p, q, r). Detailed derivations of the aircraft equations of motion are available in flight dynamics textbooks, such as [9].

Longitudinal dynamics

A 6 degrees-of-freedom (Longitudinal and Lateral) non-linear model of the UAV was built in Simulink. Inorder to apply linear controller law, a linear model is required.

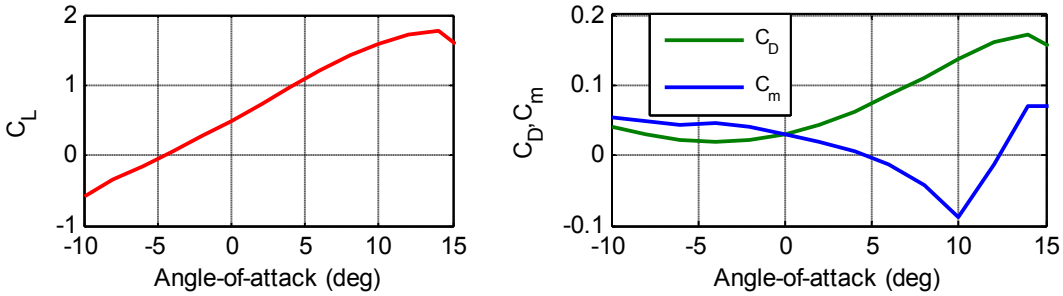

Fig. 2. Longitudinal aerodynamic coefficient plot

$$
\begin{aligned}
&m\dot{u} - \tilde{X}_{\dot{w}}\dot{w} - \tilde{X}_{u}u - \tilde{X}_{w}w - \left(\tilde{X}_{q} - mW_{e}\right)q + mg\theta\cos\theta_{e} = \tilde{X}_{\eta}\eta + \tilde{X}_{\tau}\tau,\\
&\left(m - \tilde{Z}_{\dot{w}}\right)\dot{w} - \tilde{Z}_{u}u - \tilde{Z}_{w}w - \left(\tilde{Z}_{q} + mU_{e}\right)q + mg\theta\sin\theta_{e} = \tilde{Z}_{\eta}\eta + \tilde{Z}_{\tau}\tau,\\
&-\tilde{M}_{\dot{w}}\dot{w} + I_{y}\dot{q} - \tilde{M}_{u} - \tilde{M}_{w}w - \tilde{M}_{q}q = \tilde{M}_{\eta}\eta + \tilde{M}_{\tau}\tau,\\
&\dot{\theta} = q\cos\phi - r\sin\phi.
\end{aligned}
\tag{2}
$$

The longitudinal flight dynamics of fixed-wing aircraft are described by the set of states given as $x = (u, w, q, \theta)^{T}$, which include body x-axis velocity u(*m*/*s*), body z-axis velocity w(*m*/*s*), pitch rate q(*rad*/*s*), and pitch angle θ (*rad*). The primary control surface input in this longitudinal dynamics model is the elevator deflection η (rad). The linear longitudinal dynamics of a fixed-wing UAV can be represented as given in (2); axial force *X*, normal force, *Z, pitching* moment *M* and kinematic dynamic equation respectively.

The terms, *We*, *Ue* and *θe* represent equilibrium values and depend on the selected operating points for which the linear model is generated. A trim condition needs to be imposed, before linearization of the non-linear model around the trim conditions. A steady state trimmed flight condition is found from the non-linear model. The flight conditions imposed in the model are: *u=17m/s, v=0, w=0.369m/sec, α= θ= 0.0217rad, p= q= r= 0* and *η= 0.091, τ =0.559, h=120m, mass=2.15kg.* The linearized longitudinal equations of motion in state space can be represented as

$$
\begin{bmatrix}\dot{u}\\ \dot{w}\\ \dot{q}\\ \dot{\theta}\end{bmatrix} = \begin{bmatrix}x_{u} & x_{w} & x_{q} & x_{\theta}\\ z_{u} & z_{w} & z_{q} & z_{\theta}\\ m_{u} & m_{w} & m_{q} & m_{\theta}\\ 0 & 0 & 1 & 0\end{bmatrix}\begin{bmatrix}u\\ w\\ q\\ \theta\end{bmatrix} + \begin{bmatrix}x_{\eta} & x_{\tau}\\ z_{\eta} & z_{\tau}\\ m_{\eta} & m_{\tau}\\ 0 & 0\end{bmatrix}\begin{bmatrix}\eta\\ \tau\end{bmatrix}, \tag{3}
$$

where thatx_u, z_u and $m_u$are the dimensionless stability aerodynamic derivatives with respect to the state variable *u*.While x_η, z_η and m_η are the dimensionless control aerodynamic derivatives, and $\tau(t)$ is the thrust. If the UAV's cruise speed is constant, then $\tau = 0$. Thus altitude can be controlled using the elevator η. The plant matrix in (3) can be modified to reflect the dimensional velocity perturbations u/u_0 *and* $\alpha = w/u_0$. For this study, the mini UAV pitch model is given as

$$
\dot{x} = \begin{bmatrix}-0.7401 & 0.646 & -0.028 & -0.5752\\ -0.6393 & -9.281 & 1.262 & -0.0131\\ 18.377 & -170.68 & -21.35 & 0\\ 0 & 0 & 1 & 0\end{bmatrix}\begin{bmatrix}u/u_{0}\\ \alpha\\ q\\ \theta\end{bmatrix} + \begin{bmatrix}0.74\\ -4.52\\ -244.2\\ 0\end{bmatrix}\eta \tag{4}
$$

The characteristic equation is given by (5) and the roots are given by (6)

$$
|A - \lambda I| = \lambda^{4} + 31.37\lambda^{3} + 437.15\lambda^{2} + 316.07\lambda \tag{5}
$$

$$
\lambda = \begin{bmatrix}-15.32 \pm 13.4i & -0.37 \pm 0.499i\end{bmatrix}^{T}. \tag{6}
$$

For steady-state analysis, the *DC* gain matrix of the UAV is as given in (7) and from (6), we know that the open-loopsystem is stable but from Fig. 3, the closed-loop system will be unstable. Hence, the need to design a controller is inevitable.

$$
\begin{aligned}
k &= -CA^{-1}B,\\
&= \begin{bmatrix}5.3982 & -0.8495 & 0 & -6.6134\end{bmatrix}^{T}.
\end{aligned}
\tag{7}
$$

1.3 LQG Control

By combining the solutions to the Linear Quadratic Regulator (*LQR)* and the Linear Quadratic Estimator (*LQE*) problems, we can obtain a solution to the Linear Quadratic Gaussian optimal control problem.

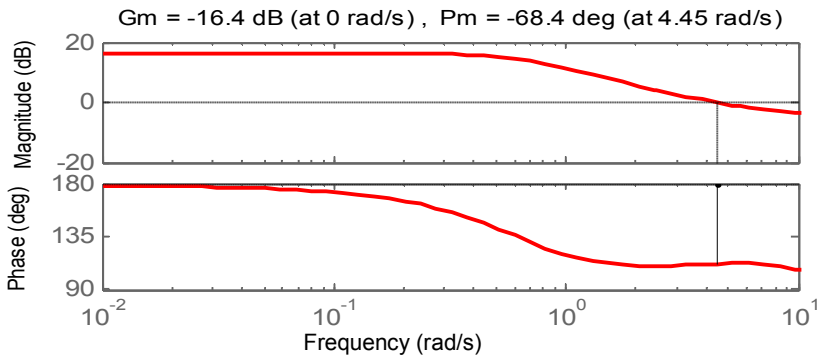

Fig. 3. Bode plot of the open-loop UAV

The *LQG* problem considers a linear system with disturbance. The noise signals have stochastic models. To emphasize this fact, [10] we write the system equations as

$$\dot{x} = Ax + Bu + Gw, \quad x \in \mathbb{R}^n, \quad u \in \mathbb{R}^p \tag{8}$$

$$y_m = Cx + v, \quad y \in \mathbb{R}^q, \quad x(t_0) = x_0, \tag{9}$$

Where v and *w*are stationary, zero mean, Gaussian white noise processes whose statistics satisfy (10) and (11). And $x_0$is a Gaussian random variable with mean $E\{x_0\} = \bar{x}_0$ and covariance that satisfies (12)-(14).*G* is the process disturbance

$$E\left\{v(t)v(\tau)^T\right\} = V\delta(t-\tau) \tag{10}$$

$$E\left\{w(t)w(\tau)^T\right\} = W\delta(t-\tau). \tag{11}$$

Note, $v(t)$, $w(t)$, and $x(t_0)$ are mutually uncorrelated sensor noise of the plant and measurements of the sensors respectively.

$$E\left\{v(t)w(\tau)^T\right\} = 0, \forall t, \tau \tag{12}$$

$$E\left\{x(t_0)v(t)^T\right\} = 0, \forall t \tag{13}$$

$$E\left\{x(t_0)w(t)^T\right\} = 0, \forall t \tag{14}$$

For this study, the following values for the sensors covariance matrices were adopted [11] and atmospheric disturbance to the plant *G* is assumed to be absent.

$$W = diag\left(\begin{bmatrix}0.01 & 0.01 & 0.01 & 0.01\end{bmatrix}\right), \quad V = 0.01. \tag{15}$$

Suppose that we wish to minimize the expected value of a quadratic cost function

$$J(t_0, x_0, u) = \lim_{x\to\infty}\frac{1}{T}E\left\{\int_0^T \left(x^TQx + u^TRu\right)dt\right\}, \tag{16}$$

where $Q \geq 0$ and $R > 0$, and the following values were adopted using Bryson's rule

$$Q = diag\left(\begin{bmatrix}0.0365 & 0.000025 & 8.2 & 0.672\end{bmatrix}\right), \quad R = 0.1. \tag{17}$$

Assume that the system dynamics, weighting matrices, and covariance matrices satisfy:

(i) (*A*,*B*) is *controllable*
(ii) (*A*,*C*) is *observable*

Then the optimal control has the form of state feedback applied to the state estimate $\hat{x}$ given by:

$$u(t) = -K\hat{x}(t), \tag{18}$$

Where

$$K = R^{-1}B^TX. \tag{19}$$

In (19), *X* is the unique positive semi-definite solution to the Algebraic Riccati Equation

$$XA + A^TX + Q - XBR^{-1}B^TX = 0 \tag{20}$$

MATLAB function *[K, X, E] = lqr (A, B,Q, R)* was use to solve (20). Hence the appropriate *LQR*

gainmatrix *K*, with the associated covariance matrix *X,* for the situation at hand was obtained. The corresponding closed-loop eigen values *E*, is -2211.3, -6.1, -0.7 and -0.3.

$$K=\begin{bmatrix}-0.0445 & 0.6829 & -8.9688 & -2.6160\end{bmatrix}, \quad (21)$$

$$X=\begin{bmatrix}0.0282 & -0.0008 & 0.0001 & -0.0107\\ -0.0008 & 0.0040 & -0.0004 & -0.0008\\ 0.0001 & -0.0004 & 0.0037 & 0.0011\\ -0.0107 & -0.0008 & 0.0011 & 2.3647\end{bmatrix}. \quad (22)$$

Kalman filter is the observer that is used in this study to estimate the states of the dynamic system. It admits the form

$$\dot{\hat{x}} = A\hat{x} + Bu + L\left(y - \hat{y}\right), \quad (23)$$

Wherethe estimated state of the observer is $\hat{x}$, with measured output as $\hat{y}$ and the observer gain *L*given as

$$L = YCW^{-1}, \quad (24)$$

with, *Y* ,the unique positive semi-definite solution to the dual Algebraic Riccati Equation:

$$0 = YA^T + AY + V - YC^TW^{-1}CY. \quad (25)$$

To solve (25) the MATLAB command *[L,Y,E]* = *lqe(A,W,C,W,V,E0)*was used,[12]. The following values of process and observation noise covariance matrices were used;

$$V = diag\left(\begin{bmatrix}0.01 & 0.01 & 0.01 & 0.01\end{bmatrix}\right),$$
$$W = diag\left(\begin{bmatrix}0.01 & 0.01 & 0.01 & 0.01\end{bmatrix}\right). \quad (26)$$

The values in (27) were obtained as the *Kalman gain* and covariance matrix. The estimator closed-loop eigenvalues are *E= -15.2558 ± 13.6429 and -0.7312 ± 0.4161i.*

$$L=\begin{bmatrix}0.1069 & 0.0026 & 0.0605 & -0.0701\\ 0.0026 & 0.0089 & -0.0193 & -0.0021\\ 0.0605 & -0.0193 & 0.2127 & -0.0329\\ -0.0701 & -0.0021 & -0.0329 & 0.2744\end{bmatrix}, \quad Y=\begin{bmatrix}0.001 & 0.0 & 0.0006 & -0.0007\\ 0.0 & 0.0001 & -0.0002 & -0.0\\ 0.0006 & -0.0002 & 0.0021 & -0.0003\\ -0.0007 & -0.0 & -0.0003 & 0.0027\end{bmatrix}. \quad (27)$$

The state estimator was designed using the *Kalman gain* obtained in (27) and the simulation results are shown in Fig. 4. Kalman filter estimates the states of the dynamic system and minimizes the error as expected and all states converge to the constant values of the *DC gain* of the open-loop system. Thus, it is an optimal observer and well established in literature. The covariance matrix of the Kalman filter is very informative; noting the fact that the diagonal elements are small for all the estimated states.

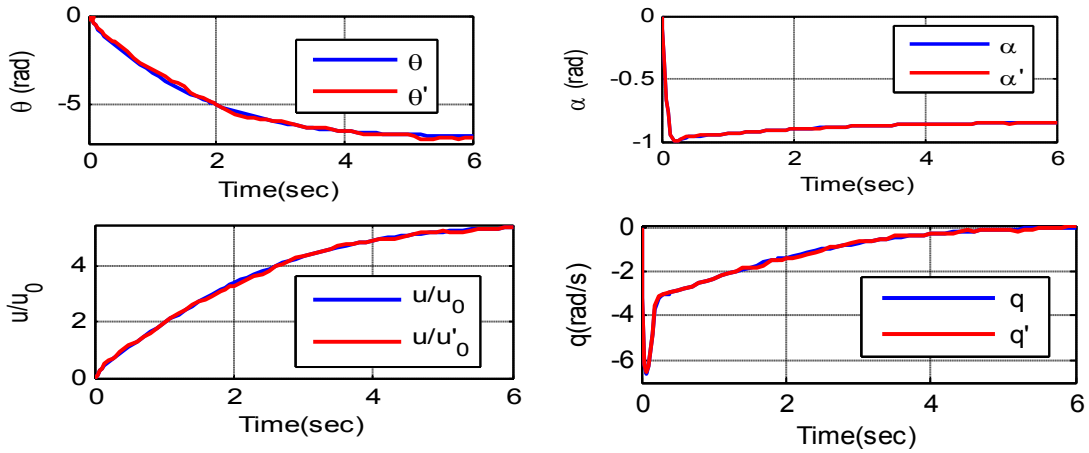

Fig. 4. Kalman filter estimate of the UAV states

It is necessary to bring to light the theoretical fact that *LQR* and Kalman filter have guaranteed robustness properties but the combination of both could elude such properties. We chose to use the robustness properties of Kalman filter in this study as the benchmark for assessing the robustness of *LQG* control algorithm and this is depicted in Fig. 5.

The separation principle makes it clear that the Kalman filter design does not depend on the weighting matrices *Q* and *R*, nor does the optimal state feedback gain depend on the noise statistics. Hence, the state equation given in matrix for the *LQG* solution is given as [13]

$$\begin{bmatrix}\dot{x}\\ \dot{e}\end{bmatrix}=\begin{bmatrix}A-BK & BK\\ 0 & A-LC\end{bmatrix}\begin{bmatrix}x\\ e\end{bmatrix}+\begin{bmatrix}B\\ 0\end{bmatrix}r,$$
$$y=\begin{bmatrix}C & 0\end{bmatrix}\begin{bmatrix}x\\ e\end{bmatrix}, \tag{28}$$

Where *e* is the error of estimated state and *r* the reference signal.

1.4 The Improved LQG Control

The traditional *LQG* requires the solution of *Algebraic Riccati Equation* (ARE) to obtain a constant value of *Kalman* gain which is used to estimate the state of the system and hence the *LQG* control scheme. Here we choose to solve the differential form of (25) as presented in (29); an Initial Value Problem (IVP). The result is an array of *Kalman* gains up to 6671 values as it tries to converge to a constant value after 10 seconds of simulation. [14].

$$\dot{Y}=YA^{T}+AY+V-YC^{T}W^{-1}CY,$$
$$Y(t_0)=diag\left(\begin{bmatrix}0.0001 & 0.0001 & 0.0001 & 0.0001\end{bmatrix}\right). \tag{29}$$

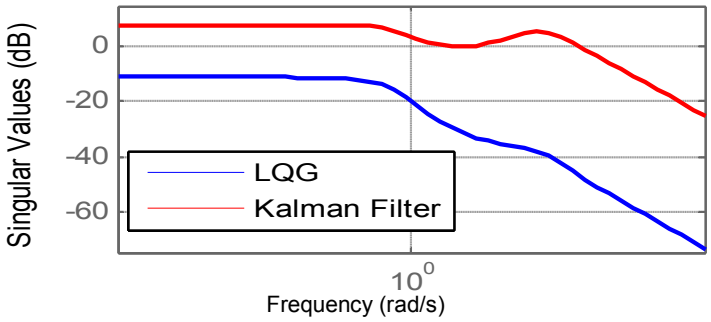

Fig. 5. SV plot for *LQG* control and Kalman filter based observer

In MATLAB/Simulink, (29) was model and incorporated as the Kalman filter design and simulated for 10 seconds. Ensuring that the set-point *LQG* tracking control scheme simulation also converges to a *steady-state* value after simulation, three ponts were selected. These points are t_1=0.5s (341th*step*), t_2=1.5 (1007th*step*) and t_3=10sec (66771th*step*). Thus, we harvested at these times of interest three contant gain matrices of *Kalman* gain and their associated covariance matrices. These are:

$$L_{i_1}=\begin{bmatrix}0.3179 & 0.0083 & 0.1499 & -0.0436\\ 0.0083 & 0.0340 & -0.1339 & -0.0041\\ 0.1499 & -0.1339 & 1.1861 & 0.0501\\ -0.0436 & -0.0041 & 0.0501 & 0.5138\end{bmatrix},\ Y_{i_1}=\begin{bmatrix}0.0032 & 0.0001 & 0.0015 & -0.0004\\ 0.0001 & 0.0003 & -0.0013 & -0.0000\\ 0.0015 & -0.0013 & 0.0119 & 0.0005\\ -0.0004 & -0.0000 & 0.0005 & 0.0051\end{bmatrix}, \tag{30}$$

$$L_{i_2}=\begin{bmatrix}0.4392 & 0.0117 & 0.2258 & -0.1271\\ 0.0117 & 0.0341 & -0.1318 & -0.0060\\ 0.2258 & -0.1318 & 1.2337 & -0.0010\\ -0.1271 & -0.0060 & -0.0010 & 0.9247\end{bmatrix},\ Y_{i_2}=\begin{bmatrix}0.0044 & 0.0001 & 0.0023 & -0.0013\\ 0.0001 & 0.0003 & -0.0013 & -0.0001\\ 0.0023 & -0.0013 & 0.0123 & -0.0000\\ -0.0013 & -0.0001 & -0.0000 & 0.0092\end{bmatrix}, \tag{31}$$

$$L_{i_3} = \begin{bmatrix} 0.4543 & 0.0122 & 0.2356 & -0.1473 \\ 0.0122 & 0.0342 & -0.1315 & -0.0065 \\ 0.2356 & -0.1315 & 1.2398 & -0.0136 \\ -0.1473 & -0.0065 & -0.0136 & 0.9752 \end{bmatrix}, \; Y_{i_3} = \begin{bmatrix} 0.0045 & 0.0001 & 0.0024 & -0.0015 \\ 0.0001 & 0.0003 & -0.0013 & -0.0001 \\ 0.0024 & -0.0013 & 0.0124 & -0.0001 \\ -0.0015 & -0.0001 & -0.0001 & 0.0098 \end{bmatrix}. \quad (32)$$

Thus, the improved Kalman gains. The observer poles with respect to the improved *Kalman* gains L_{ij} ,where *j=1..3,* are as follows: E_{i1}= -15.7373 ± 14.1620*i* , -0.9742 ± 0.3560*i* , E_{i2}=-15.737 ± 14.1623*i* , -0.9742 ± 0.4720*i*, and E_{i3}= -15.7374 ± 14.1621*i* , -1.2999 ± 0.4789*i*.

The *Kalman* gain matrices in (30), (31) and (32) were used in the design of the controllers,LQG_{i1}, LQG_{i2} and LQG_{i3} respectively. Set-point tracking of θ=0.026*rad*control simulation of the respective controllers gave the result in Fig. 6. To simulate the effect of external disturbance on the controllers designed, *Band-Limited-White-Noise* block in Simulink/MATLAB®was used. First, a noise power of 10^{-6} was selected to accertain the robustness of the controllers synthesied. This was incooperated in the set-point tracking simulation scenerio.

After running the simulation for 100 seconds the results for all controllers synthesised are as shown in Fig. 7. When the noise power was increased to 0.01 and simulating for 150second, Fig. 8 depicts a comparison plot between LQG_{i3} and *LQG* controller.

To further investigate the robustness properties of the all four controllers in this study, the need for a Singular Value (SV) is invalueable. Since the bases for evaluating this robustness is the Kalman filter, we intend to have four SV plots, these are captured in Fig. 9.

2. Discussion of Result

It is obvious that from Fig. 6, that not much disperity is seen in the *step response* characteristics of all four controllers synthersied. A *steady-state-error* (SSE) of 0.001 is prevalent will all controllers, which is acceptable for prilimenary design.*Rise time*, and *settling time* are about the same for all controllers. Also, no *overshoot* is observed.

When external disturbance is model as white noise and added to the system simulation, the controllers show good commad follow of the reference set-point of pitch angle of 0.026rad as dipicted in Fig. 7. Further increament in noise power gave the result in Fig. 8. Here, it could be ssen that *LQG* controller deviated further awayfrom the command set-point than the LQG_{i3}. With this results, it is still very difficult to appreciate how much the improved controllers (LQG_{ij}) perform better than the *LQG* controller.

This basic fact shows why it is necessary to always assess a controller design form stand-point of both *step response*characteristics and *gain margin (GM)*.Frequency response provides a powerful stability analysis tool.For a closed loop system to be stable, the frequency response of its open loop components must have at least a *gain margin* greater than 1 (0 *dB*). Using 0*db* gain as the minimm requirement for robustness of a system, with results from Fig 9, Table 2 gives a summary of results for furtherdiscussion.

The robustness of the *LQG* controller is lost completely from the standpoint of the *LQE* gain of 7.92db. This is expected and well established in litereture. Interestingly, three of the improved*LQG* controllers(LQG_{ij} were *j=1..3*) were able to recover the lost rubustness of the *LQG*with varying percentages as higlighted in Table 2. LQG_{i3}has the highest recovered robustnes, which is 82.5%.Typically, this means in the presence of uncertain disturbance of the same magnitude such as wind gust subjected to all four controllers and sustained for the same period of time, the *LQG* controller will lose it robustness first, followed by LQG_{i1},then LQG_{i2} and finally LQG_{i3}. This argument is supported with simulation result in Fig. 8, though comparing only the *LQG* withLQG_{i3}.

Table 2. SV plot gains

System	Gain (db)	Percentage recovered
Kalman Filter	7.92*db*	-
LQG	-11*db*	0
LQG_{i1}	-3.5*db*	68.2
LQG_{i2}	-2.034*db*	81.5
LQG_{i3}	-1.92 *db*	82.5

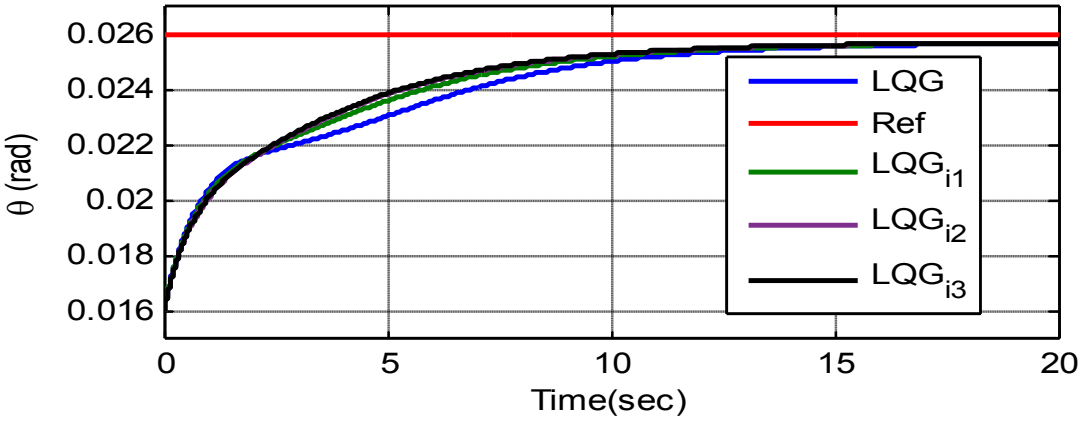

Fig. 6. LQG and improve LQG controllers Set-point tracking response

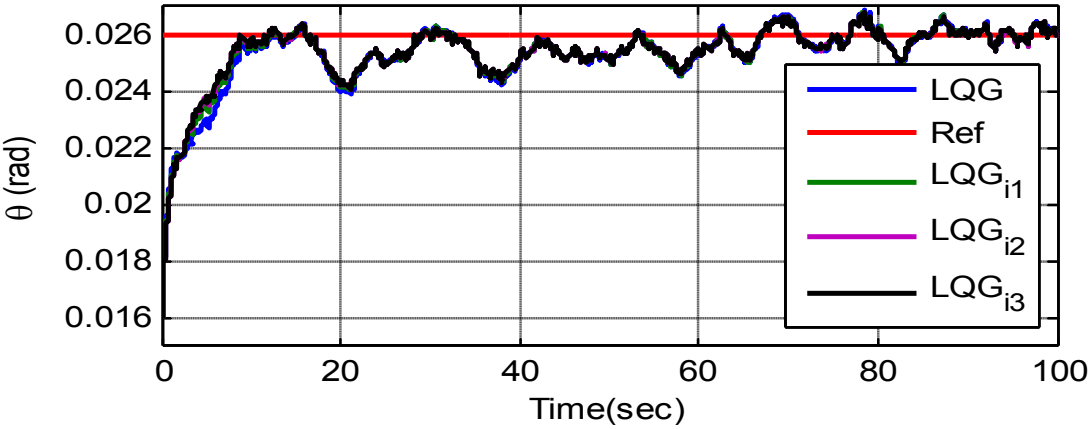

Fig. 7. Set-point tracking response with disturbance for LQG and *LQG$_{ij}$*controllers

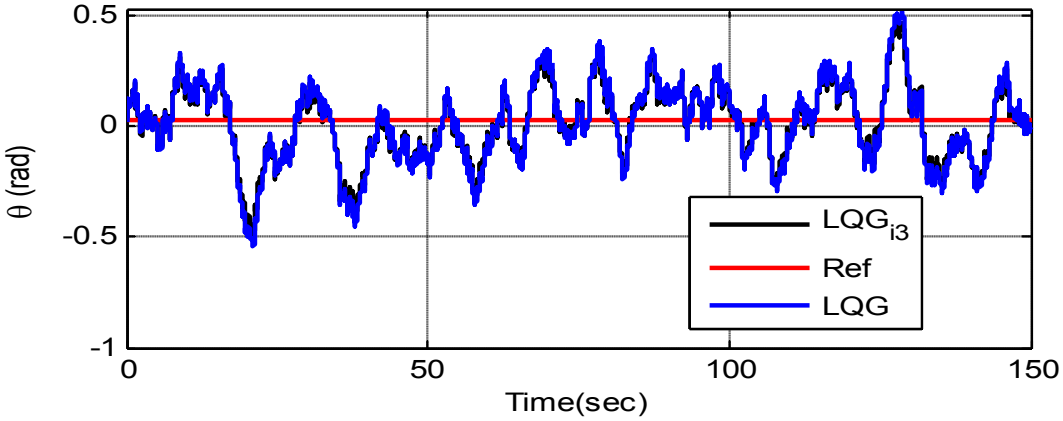

Fig. 8. Set-point tracking response with increased magnitude of disturbance for LQG and *LQG$_{i3}$* controllers

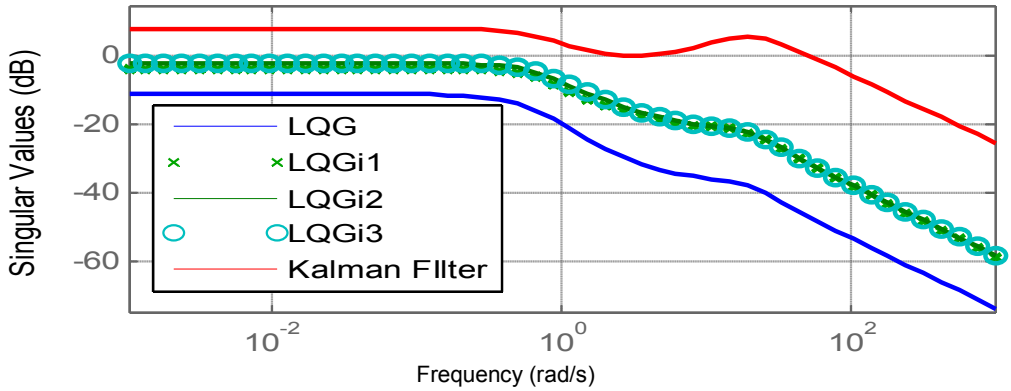

Fig. 9. Comparative SV plot of *LQG*, LQG_{ij}& Kalman filter

3. CONCLUSION

To control a mini-UAV, first detail aerodynamic modeling of the system must be done to come up with a mathematical description of the system to be controlled. In this study, Aircraft DIGITAL DATCOM® was used to achieve such feat. A longitudinal model dynamics of the UAV wasdecoupled from a six-degree-of-freedom nonlinear model of the UAV. Trimiming and linearization was necessary and was carried out in MATLAB/Simulink®. This is needed in other to design a linear based controller. Four controllers we designed in this study, the *LQG* and three other improved forms of it (LQG_{ij} were $j=1..3$). The improvement was from the standpoint of solving a *Differential Riccati Equation* (*DRE*) to obtain the required *Kalman* filter gain rather than an *AlgebraiceRiccati Equation* (*ARE*). Simulation results of all the three improved *LQG* controllersshows theirable to recover the robustness lost by the *LQG* controller. Taking 0*db* as the minimum requirement for robustness, all four controllers synthesiedhave the followingpacentages of recovered robustnes:*LQG*=0%,LQG_{i1}=68.2%,LQG_{i2}= 81.5% and LQG_{i3}=82.5%.Thus, all three improved*LQG* controllers outperformed the traditional *LQG* control algorithm both from the standpoint of *step responses*, disturbance and robustness in terms of Singular Value.

FUTURE WORK

The need to investigate that theLQG dual phenomenon holds for these improved controllers is a paramount. This willconclude the study here. It is of great interest also to investigate how much robustness can be recovered if an LQG/LTR is designed for this same system and compared with the LQG_{ij} designs presented here.

COMPETING INTERESTS

Authors have declared that no competing interests exist.

REFERENCES

1. Dongwon Jung. Hierarchical path planning and control of a small fixed-wing UAV: Theory and Experimental Validation. PhD Dissertation. Georgia Institute of Technology; 2007.
2. Ryan A, Zennaro M, Howel A, Sengupta R. Hedrick JK. An overview of emerging results cooperative UAV control, 43rd IEEE Conference on Decision and Control, December 14-17, Atlantis, Paradise Island, Bahamas; 2004.
3. Borkar V, Mitter S. LQG control with communication constraints communication, computation, control, and signal processing: A tribute to Thomas kailath. Norwell, MA: kluwer; 1997.
4. Tatikonda S, Sahai A, Mitter S. Stochastic linear control over a communication channel. IEEE Transactions on Automatic Control. 2004;49(9):1549-1561.
5. Aliyu BK, Osheku CA, Oyedeji EO. Improved LQG Control System Design for Longitudinal Flight Dynamics of a Fixed-Wing UAV Autopilot. 65rd International Astronautical Congress, Toronto, Canada. International Astronautical Federation; 2004. IAC-14,B6,4-YPVF.1.1x21008
6. Taylor B, Dorobantu A, Balas G. University of Minnesota UAV Research Group. Available: http://www.uav.aem.umn.edu

7. Datcom+ Pro Users Manual Version 3.1; 2011. Holy Cows, Inc. 3757 Lake Drawdy Driv Orlando, FL 32820.
8. Houghton EL, Carpenter PW. Aerodynamics for Engineering Students; 2003. ISBN 0750651113.
9. Cook M. Flight Dynamics Principles, Elsevier Ltd. 2nd edition; 2007.
10. Huibert Kwakernaak, Raphael Sivan. Linear Optimal Control Systems. John Wiley & Sons, Inc; 1972. ISBN 0-471-51110-2.
11. Balázs Kulcsar. LQG/LTR Controller Design for An Aircraft Model. Periodica Polytechnica SER. TRANSP. ENG. 2000;28(1–2):131–142.
12. Ashish Tewari. Advance control of aircraft, spacecraft and rockets. John wiley & Sons, Ltd; 2011. ISBN 978-0-470-74563-2.
13. Huibert Kwakernaak, Raphael Sivan. Linear Optimal Control Systems. John Wiley & Sons, Inc; 1972. ISBN 0-471-51110-2.
14. Aliyu B. Kisabo, Charles A, Osheku, Adetoro M. Lanre A, Aliyu Funmilayo Adebimpe. Optimal Solution to Matrix Riccati Equation, For Kalman Filter Implementation, MATLAB – A Fundamental Tool for Scientific Computing and Engineering Applications, INTECH. 2012;3. ISBN 978-953-51-0752-1.

Peer-review history:
The peer review history for this paper can be accessed here:
http://www.sciencedomain.org/review-history.php?iid=757&id=31&aid=7062